patient was similar to that observed in FLCs. The three possible explanations as to why FLCs remained in our case are as follows: Firstly, *NR5A1* may control target gene (s) that determine the fate of FLCs. Second, cells are more visible because of fat accumulation in the cytoplasm. Indeed, Camats *et al.*[26] reported vacuolization of Leydig cells in 2-year-old patients because of fat accumulation. Third, FLC hyperplasia is possible owing to increased secretion of HCG by the placenta and foetal pituitary LH. Ogata[34] reported that Leydig cells had increased in number and were swollen with abundant lipoid material in the testes at the age of 14 months in a patient with congenital lipoid adrenal hyperplasia. This report supports the second and third hypotheses. The mechanistic details leading to residual FLC accumulation remain to be elucidated.

Conclusions

We have described two families with novel heterozygous *NR5A1* mutations, D257TfsX39 and V424del. The 46,XY mutation carriers had severe submasculinization. The 46,XX mutation carriers showed primary ovarian insufficiency. Our experience suggests that anxiety and/or depression might be psychiatric symptoms of 46,XX mutation carriers. Psychiatric symptoms in human *NR5A1* mutation carriers should be elucidated, not only in affected members but also in as many other family members as possible.

Acknowledgements

We are extremely grateful to Prof. Takao Takahashi for the fruitful discussions. We also thank Dr. Toshihiko Yanase for providing the CYP19A1-luc reporter, Dr. Maki Fukami for providing the plasmid containing *NR5A1* cDNA and the CYP11A1-luc reporter, Dr. Kenichiro Morohashi for providing the Ad4BP (NR5A1) antibody and Ms. Fumiko Kato for her technical assistance.

This work was supported in part by a Grant from the Ministry of Health, Labour and Welfare of Japan (grant number: Jitsuyoka (Nanbyo) – Ippan – 014).

Disclosures

All the authors declare that they are not aware of any potential financial or other conflict of interest related to this work.

References

1 Luo, X., Ikeda, Y. & Parker, K.L. (1994) A cell-specific nuclear receptor is essential for adrenal and gonadal development and sexual differentiation. *Cell*, **77**, 481–490.

2 Zhao, L., Bakke, M. & Parker, K.L. (2001) Pituitary-specific knockout of steroidogenic factor 1. *Molecular and Cellular Endocrinology*, **185**, 27–32.

3 Jeyasuria, P., Ikeda, Y., Jamin, S.P., *et al.* (2004) Cell-specific knockout of steroidogenic factor 1 reveals its essential roles in gonadal function. *Molecular Endocrinology*, **18**, 1610–1619.

4 Lourenco, D., Brauner, R., Lin, L., *et al.* (2009) Mutations in NR5A1 associated with ovarian insufficiency. *The New England Journal of Medicine*, **360**, 1200–1210.

5 Yokoya, S. (1983) Measurement of Penile and clitoral size in pre-term and term newborns, infants, and children; toward earlier recognition of congenital endocrine disorders. *Clinical Endocrinology*, **31**, 1215–1220.

6 Ito, J., Tanaka, T., Horikawa, R., *et al.* (1993) Clinical study on the time-resolved fluoroimmunoassay of Serum luteinizing hormone and follicle stimulating hormone in children: The change of serum gonadotropins in LHRH test and night time secretion during puberty. *Journal of Japan Pediatric Society*, **97**, 1789–1796.

7 Winter, J.S., Taraska, S. & Faiman, C. (1972) The hormonal response to HCG stimulation in male children and adolescents. *The Journal of Clinical Endocrinology and Metabolism*, **34**, 348–353.

8 Sakakura, K. & Kohhka, K. (2005) Menopause woman's reference range of hypophysis and sex hormone using automatic electrochemiluminescence immunoassay analyzer "Modular Analytics". *Clinical Endocrinology*, **53**, 545–551.

9 Anasti, J. (1998) Premature ovarian failure: an update. *Fertility and Sterility*, **70**, 1–15.

10 Fujieda, K. & Matsuura, N. (1987) Growth and maturation in the male genitalia from birth to adolescence. I. Change of testicular volume. *Acta Paediatrica Japonica*, **29**, 214–219.

11 Matsuo, N., Anzo, M., Sato, S., *et al.* (2000) Testicular volume in Japanese boys up to the age of 15 years. *European Journal of Pediatrics*, **159**, 843–845.

12 Achenbach, T.M. & Rescorla, L.A., ed. (2001) Manual for the ASEBA School-Age Forms and Profiles. University of Vermont, Research Center for Children, Youth, and Families, Burlington, VT.

13 Beck, A.T., Ward, C.H., Mendelson, M., *et al.* (1961) An inventory for measuring depression. *Archives of General Psychiatry*, **4**, 561–571.

14 Yokoyama, C., Komatsu, T., Ogawa, H., *et al.* (2009) Generation of rat monoclonal antibodies specific for Ad4BP/SF-1. *Hybridoma (Larchmt)*, **28**, 113–119.

15 Bates, P.A., Kelly, L.A. & MacCallum, R.M., *et al.* (2001) Enhancement of protein modeling by human intervention in applying the automatic programs 3D-JIGSAW and 3D-PSSM. *Proteins*, **45**, 39–46.

16 Hasegawa, T. (2004) Testicular dysgenesis without adrenal insufficiency in a 46,XY patient with a heterozygous inactive mutation of steroidogenic factor-1. *The Journal of Clinical Endocrinology and Metabolism*, **89**, 5930–5935.

17 Oba, K., Yanase, T., Nomura, M., *et al.* (1996) Structural characterization of human Ad4bp (SF-1) gene. *Biochemical and Biophysical Research Communications*, **226**, 261–267.

18 Zhao, L., Kim, K.W., Ikeda, Y., *et al.* (2008) Central nervous system-specific knockout of steroidogenic factor 1 results in increased anxiety-like behavior. *Molecular Endocrinology*, **22**, 1403–1415.

19 Kim, K.W., Zhao, L. & Parker, K.L. (2009) Central nervous system-specific knockout of steroidogenic factor 1. *Molecular and Cellular Endocrinology*, **300**, 132–136.

20 Achermann, J.C., Ozisik, G., Ito, M., *et al.* (2002) Gonadal determination and adrenal development are regulated by the orphan nuclear receptor steroidogenic factor-1, in a dose-dependent manner. *The Journal of Clinical Endocrinology and Metabolism*, **87**, 1829–1833.

21 Coutant, R., Mallet, D., Lahlou, N., *et al.* (2007) Heterozygous mutation of steroidogenic factor-1 in 46,XY subjects may mimic partial androgen insensitivity syndrome. *The Journal of Clinical Endocrinology Metabolism*, **92**, 2868–2873.

22 Philibert, P., Zenaty, D., Lin, L., *et al.* (2007) Mutational analysis of steroidogenic factor 1 (NR5a1) in 24 boys with bilateral anorchia: a French collaborative study. *Human Reproduction*, **22**, 3255–3261.

23 Warman, D.M., Costanzo, M. & Marino, R., *et al.* (2011) Three new SF-1 (NR5A1) gene mutations in two unrelated families with multiple affected members: within-family variability in 46, XY subjects and low ovarian reserve in fertile 46,XX subjects. *Hormone Research in Paediatrics*, **75**, 70–77.

24 Janse, F., de With, L.M., Duran, K.J., *et al.* (2012) Limited contribution of NR5A1 (SF-1) mutations in women with primary ovarian insufficiency (POI). *Fertility and Sterility*, **97**, 141–146.e142.

25 Kohler, B., Lin, L., Ferraz-de-Souza, B., *et al.* (2008) Five novel mutations in steroidogenic factor 1 (SF1, NR5A1) in 46,XY patients with severe underandrogenization but without adrenal insufficiency. *Human Mutation*, **29**, 59–64.

26 Camats, N.P.A., Fernández-Cancio, M., Andaluz, P., *et al.* (2012) Ten novel mutations in the NR5A1 gene cause disordered sex development in 46,XY and ovarian insufficiency in 46,XX individuals. *The Journal of Clinical Endocrinology and Metabolism*, **97**, E1294–E1306.

27 Lin, L., Philibert, P., Ferraz-de-Souza, B., *et al.* (2007) Heterozygous missense mutations in steroidogenic factor 1 (SF1/Ad4BP, NR5A1) are associated with 46,XY disorders of sex development with normal adrenal function. *The Journal of Clinical Endocrinology and Metabolism*, **92**, 991–999.

28 Allali, S., Muller, J.B., Brauner, R., *et al.* (2011) Mutation analysis of NR5A1 encoding steroidogenic factor 1 in 77 patients with 46, XY disorders of sex development (DSD) including hypospadias. *PLoS ONE*, **6**, e24117.

29 Johannsen, T.H., Ripa, C.P., Mortensen, E.L., *et al.* (2006) Quality of life in 70 women with disorders of sex development. *European Journal of Endocrinology*, **155**, 877–885.

30 Kohler, B., Lin, L., Mazen, I., *et al.* (2009) The spectrum of phenotypes associated with mutations in steroidogenic factor 1 (SF-1, NR5A1, Ad4BP) includes severe penoscrotal hypospadias in 46,XY males without adrenal insufficiency. *European Journal of Endocrinology*, **161**, 237–242.

31 Codesal, J., Regadera, J., Nistal, M., *et al.* (1990) Involution of human fetal Leydig cells. An immunohistochemical, ultrastructural and quantitative study. *Journal of Anatomy*, **172**, 103–114.

32 Prince, F.P. (1984) Ultrastructure of immature Leydig cells in the human prepubertal testis. *The Anatomical Record*, **209**, 165–176.

33 Cools, M., Hoebeke, P., Wolffenbuttel, K.P., *et al.* (2012) Pubertal androgenization and gonadal histology in two 46,XY adolescents with NR5A1 mutations and predominantly female phenotype at birth. *European Journal of Endocrinology*, **166**, 341–349.

34 Ogata, T., Matsuo, N., Saito, M., *et al.* (1989) The testicular lesion and sexual differentiation in congenital lipoid adrenal hyperplasia. *Helvetica Paediatrica Acta*, **43**, 531–538.

35 Ogata, T., Matsuo, N., Saito, M., *et al.* (1989) The testicular lesion and sexual differentiation in congenital lipoid adrenal hyperplasia. *Helvetica Paediatrica Acta* **43**, 531–538.

OPEN ACCESS Freely available online

PLOS ONE

Quantitative and Sensitive Detection of *GNAS* Mutations Causing McCune-Albright Syndrome with Next Generation Sequencing

Satoshi Narumi[1☯]*, Kumihiro Matsuo[2☯], Tomohiro Ishii[1], Yusuke Tanahashi[2], Tomonobu Hasegawa[1]

1 Department of Pediatrics, Keio University School of Medicine, Tokyo, Japan, **2** Department of Pediatrics, Asahikawa Medical University, Hokkaido, Japan

Abstract

Somatic activating *GNAS* mutations cause McCune-Albright syndrome (MAS). Owing to low mutation abundance, mutant-specific enrichment procedures, such as the peptide nucleic acid (PNA) method, are required to detect mutations in peripheral blood. Next generation sequencing (NGS) can analyze millions of PCR amplicons independently, thus it is expected to detect low-abundance *GNAS* mutations quantitatively. In the present study, we aimed to develop an NGS-based method to detect low-abundance somatic *GNAS* mutations. PCR amplicons encompassing exons 8 and 9 of *GNAS*, in which most activating mutations occur, were sequenced on the MiSeq instrument. As expected, our NGS-based method could sequence the *GNAS* locus with very high read depth (approximately 100,000) and low error rate. A serial dilution study with use of cloned mutant and wildtype DNA samples showed a linear correlation between dilution and measured mutation abundance, indicating the reliability of quantification of the mutation. Using the serially diluted samples, the detection limits of three mutation detection methods (the PNA method, NGS, and combinatory use of PNA and NGS [PNA-NGS]) were determined. The lowest detectable mutation abundance was 1% for the PNA method, 0.03% for NGS and 0.01% for PNA-NGS. Finally, we analyzed 16 MAS patient-derived leukocytic DNA samples with the three methods, and compared the mutation detection rate of them. Mutation detection rate of the PNA method, NGS and PNA-NGS in 16 patient-derived peripheral blood samples were 56%, 63% and 75%, respectively. In conclusion, NGS can detect somatic activating *GNAS* mutations quantitatively and sensitively from peripheral blood samples. At present, the PNA-NGS method is likely the most sensitive method to detect low-abundance *GNAS* mutation.

Citation: Narumi S, Matsuo K, Ishii T, Tanahashi Y, Hasegawa T (2013) Quantitative and Sensitive Detection of *GNAS* Mutations Causing McCune-Albright Syndrome with Next Generation Sequencing. PLoS ONE 8(3): e60525. doi:10.1371/journal.pone.0060525

Editor: Joseph Devaney, Children's National Medical Center, United States of America

Received October 2, 2012; **Accepted** February 28, 2013; **Published** March 25, 2013

Funding: This work was supported by the Grant-in-Aid for Young Scientists (B) (24791087) from the Japan Society for the Promotion of Science, and the Health Science Research Grant for Research on Applying Health Technology [Jitsuyoka (Nanbyo)-Ippan-014] from the Ministry of Health, Labour and Welfare, Japan. The funders had no role in study design, data collection and analysis, decision to publish, or preparation of the manuscript.

Competing Interests: The authors have declared that no competing interests exist.

* E-mail: sat_naru@hotmail.com

☯ These authors contributed equally to this work.

Introduction

The rapid emergence of next generation sequencing (NGS) is revolutionizing medical sciences. NGS now allows clinical investigators to analyze transcriptome, exome and genome from small amounts of DNA/RNA. NGS is also available for ultra-deep sequencing of PCR amplicons, microRNA and microbiomes. NGS-based approaches have brought remarkable advances in a broad range of medical research areas, such as studies of rare Mendelian disorders [1] and surveillance of infectious disease outbreaks [2]. NGS has also provided a wealth of new information for cancer genomics, owing in part to the ultra-deep amplicon sequencing of cancerous and precancerous cells [3]. Because NGS can analyze millions of DNA fragments simultaneously and independently, low abundance mutations of oncogenes have now become readily detectable. However, in contrast to advances in understanding of somatic mutations associated with cancer, knowledge about somatic mutations causing benign congenital disorders remains very limited.

McCune-Albright syndrome (MAS; OMIM #174800) is a rare congenital disorder hallmarked by osseous fibrous dysplasia, café-au-lait skin pigmentation and various endocrine hyperfunction, *e.g.*, peripheral precocious puberty, Cushing syndrome and functional pituitary adenoma [4,5]. MAS is caused by activating mutations of *GNAS*, encoding the stimulatory G-protein alpha subunit [6]. Mutations are exclusively present in the somatic mosaic state, probably because the nonmosaic state leads to early embryonic lethality. Clinical manifestations of MAS are highly variable in all three lesions, presumably due to variability of mutation abundance among affected tissues.

In MAS patients, mutation abundance is generally low in unaffected tissues. Thus, mutations in peripheral blood leukocytes (PBL) cannot be detected by standard PCR-based Sanger sequencing, while mutations in affected lesions (*e.g.*, surgical bone specimens) can. Based on the fact that the vast majority of activating *GNAS* mutations occurs in the Arg201 residue, Candeliere *et al.* developed the method for selective enrichment of Arg201 *GNAS* mutations using a series of nested PCR and restriction enzyme digestion [7]. Subsequently, the second enrichment method with use of a peptide nucleic acid (PNA) probe, which forms hybrids with wildtype DNA and inhibits PCR

amplification, was developed [8]. Mutation detection rate from PBL samples with these two methods are typically around 50% [9–11]. Of interest, mutation detection rate increases up to 90% when DNA sample derived from the affected lesion is available [10]. This implies that diagnostic performance of the two methods is still inadequate.

In the present study, we developed a novel NGS-based method that can detect low-abundance *GNAS* mutations quantitatively and sensitively. We compared diagnostic performance of the NGS-based method with that of the PNA method, by a serial dilution study and a mutation detection study using 16 MAS patient-derived PBL samples.

Materials and Methods

PCR with or without the PNA probe

The overview of mutation detection methods is shown in **Figure 1**. All DNA samples used in the study was extracted from PBL with the Gentra Puregene Blood Kit (Qiagen, Hilden, Germany). Partial region of the *GNAS* locus (chr20:57484398-57484647; hg19), in which nucleotides 598 to 711 (begins at the first ATG codon) were included, was PCR-amplified with or without the PNA probe. The PCR mixture (final volume 20 μL) contained 100 ng genomic DNA, 0.25 mM dNTPs, primers (0.25 μM each), and 1 U Herculase II Fusion DNA Polymerases in reaction buffer (Agilent Technologies, Santa Clara, CA), with or without 30 μM PNA probe (Panagene Inc., Daejeon, Korea). The PCR conditions were as follows: initial denaturation at 98°C for 30 s; 35 cycles at 98°C for 10 s (denaturation), 68°C for 60 s (hybridization), 55°C for 30 s (annealing) and 72°C for 30 s (extension) with a final extension at 72°C for 5 min. The sequences of the PNA and primers were as follows: PNA Gly-NH_2-CGC TGC CGT GTC-HAc; sense primer 5′-CTA CAC GAC GCT CTT CCG ATC TGT TTC AGG ACC TGC TTC GC-3′; and antisense primer 5′-GTG ACT GGA GTT CAG ACG TGT GCT CTT CCG ATC TCA CAG CAT CCT ACC GTT GAA-3′ (adaptor sequences used in Illumina platform are underlined). Generated PCR products were purified with the Agencourt AMPure XP Bead system (Beckman Coulter Genomics, Essex, UK), and were subject to both Sanger sequencing and NGS.

Mutation detection by Sanger sequencing and NGS

For Sanger sequencing, we used the BigDye Dideoxy Sequence Kit (Life Technologies, Carlsbad, CA) and the ABI3130*xl* sequencer (Life Technologies). Presence/absence of mutations was judged based on visual inspection of each sequence chromatogram.

As for NGS, we performed 15 cycles of second PCR using diluted first PCR products to add the attachment sites (P5 and P7) and the index sequence, which are used in Illumina multiplexed sequencing. The PCR mixture (final volume 20 μL) contained 1 μL purified first PCR product (diluted 1:20 with pure water), 0.25 mM dNTPs, primers (0.25 μM each), and 1 U Herculase II Fusion DNA Polymerases in reaction buffer. The PCR conditions were as follows: initial denaturation at 98°C for 30 s; 15 cycles at 98°C for 10 s, 55°C for 20 s and 72°C for 30 s with a final extension at 72°C for 5 min. The sequences of the primers were as follows: sense primer: 5'- AAT GAT ACG GCG ACC ACC GAG ATC TAC ACT CTT TCC CTA CAC GAC GCT CTT CCG ATC T-3'; and antisense primer: 5'- CAA GCA GAA GAC GGC ATA CGA GAT NNN NNN GTG ACT GGA GTT CAG ACG TGT-3' (P7 and P5 attachment sites are underlined. NNN NNN in the antisense primer denotes index-specific sequence). The second PCR products were purified with the AMPure system, and were quantified with the Qubit dsDNA HS Assay Kit (Life Technologies). In each NGS run, 16 samples were multiplexed per pool. To improve base call accuracy, an equimolar quantity of the PhiX control (Illumina, San Diego, CA) was added to the pool.

Pooled samples were pair-end sequenced on the MiSeq instrument with at least 30 cycles and an index read. Base calling, read filtering and demultiplexing were performed according to the standard Illumina processing pipeline. Sequence reads were mapped to the *GNAS* genomic sequence with Bowtie [12]. We used SAMtools to calculate read depth and nucleotide frequencies for each position of the amplicons [13]. Filtering threshold was set to Q35, which is equivalent to the probability of an incorrect base call 1 in 3160 times. For each experiment, three control PBL DNA samples were analyzed to define the experiment-specific reference upper limit of the variant call (z-score equal or more than 2.5 were defined as positive). All DNA samples were amplified and sequenced twice.

Serial dilution of cloned mutant DNAs

A first PCR product generated from an R201H mutation carrying patient was cloned into the pCR2.1-TOPO vector (Life Technologies). We prepared wildtype or mutant DNA (each 1 ng/ μL) by diluting sequence-verified plasmids. Then, we diluted cloned mutant DNA into cloned wildtype DNA to 1/10 [relative mutation abundance (RMA), 10%], 1/100 (1%), 1/333 (0.3%), 1/1,000 (0.1%), 1/3,333 (0.03%) and 1/10,000 (0.01%). Serially diluted DNA samples were subject to sequence analyses described above.

Clinical samples

In a comparative mutation detection study, 16 PBL genome samples derived from MAS patients (6 boys and 10 girls) were used. The 16 patients had classic form of MAS with two or three features of the triad (osseous fibrous dysplasia, café-au-lait skin pigmentation and endocrine hyperfunction) (**Table 1**). Fibrous dysplasia, café-au-lait skin pigmentation and endocrine hyperfunction were observed in 14 (88%), 12 (75%) and 14 (88%), respectively. Eight subjects (50%) had all three features. Observed endocrine dysfunction includes peripheral precocious puberty (N = 9), functional thyroid adenoma (N = 3), functional pituitary adenoma (N = 2) and Cushing syndrome (N = 2) (**Table 1**).

Ethics statement

The study was approved by the Institutional Review Boards of Asahikawa Medical University and Keio University School of Medicine. Written informed consent for molecular studies was obtained from the subjects or his/her parents.

Results

GNAS amplicon sequencing by NGS

We designed chimeric primer pairs, containing both locus-specific and adapter sequences, to generate PCR amplicons that are directly sequenced on the Illumina MiSeq platform. The amplicon covers two known sites of activating *GNAS* mutations (*i.e.*, Arg201 and Gln227 [14]), thus would be expected to detect most mutations causing MAS. This experimental design allowed us to generate very high read depth per sample (approximately 100,000) with low error rate (mean±SD, 0.011±0.005%) (data not shown).

Quantitative detection of a GNAS mutation

To test the ability of the NGS-based mutation detection to provide quantitative data, we conducted a serial dilution study

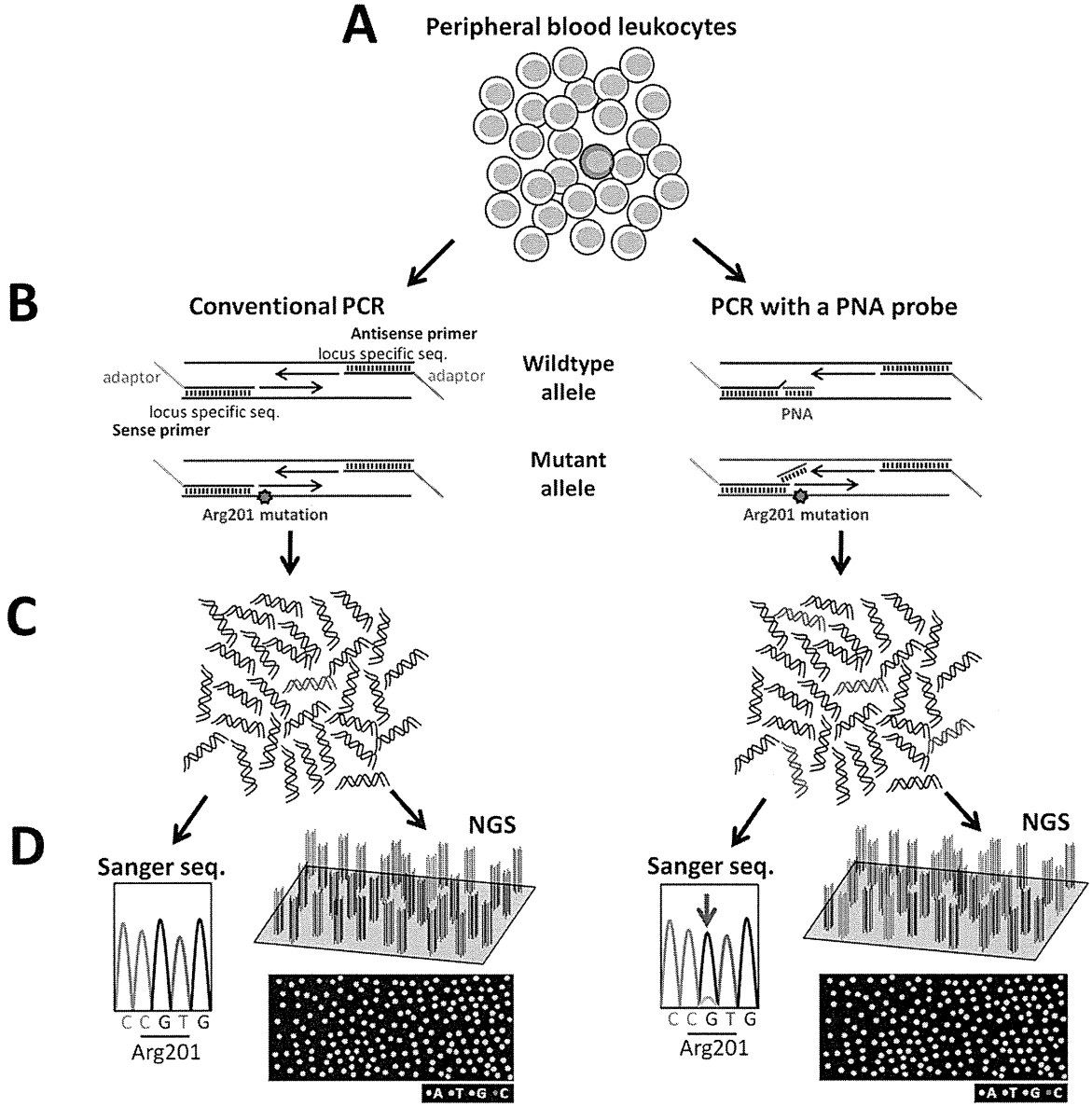

Figure 1. Schematic diagramas showing an overview of mutation detection methods. (**A**) In patients with McCune-Albright syndrome, the proportion of mutation-carrying cells (colored red) is low in peripheral blood leukocytes (PBL). (**B**) In the present study, PCR amplification was conducted in the absence (*left panel*) or presence (*right panel*) of the peptide nucleic acid (PNA) probe. The PNA probe preferentially hybridizes to wildtype PCR fragments (colored black) and inhibits their amplification. This results in enrichment of mutant PCR fragments (colored red). We used chimeric PCR primers, containing both locus-specific and adapter sequences, to generate amplicons that are sequenced on the Illumina platform. (**C**) PCR without the PNA probe produces PCR amplicons, of which relative proportion between wildtype (colored black) and mutant (colored red) is similar to PBL (*left panel*). In contrast, PNA treatment enriches mutant amplicons (*right panel*). (**D**), PCR amplicons were analyzed by both Sanger sequencing and next generation sequencing ('NGS'). Due to low mutation abundance, mutations cannot be detected in amplicons generated without the PNA probe (*left panel*), while they can be detected in PNA-treated amplicons (*right panel*, an arrow indicates the mutation). In the MiSeq platform, clonal clusters, each derived from a single DNA molecule, are generated on a flow cell, and are sequenced base-by-base simultaneously and independently. The diagrams under the schematic flow cells show imaginative optically scanned data of the cycle corresponding to the mutated nucleotide. In a sample without PNA treatment, the mutant amplicons can be recognized on the flow cell (*left panel*). Mutant-enriched samples are also analyzable by NGS (*right panel*).
doi:10.1371/journal.pone.0060525.g001

using cloned plasmid DNA samples (wildtype or R201H). We serially diluted mutant DNA into wildtype DNA, and measured mutant abundance with NGS. As we expected, a linear correlation between true mutant abundance and measured relative mutation abundance (NGS-measured RMA; defined as the proportion of sequence reads containing the mutation), was observed down to 0.01% (**Figure 2**), indicating reliable quantification.

Table 1. Characteristics of the study subjects.

ID	Sex	MAS features			Relative mutation abundance (%)	Mutation detection method		
		FD	Skin lesion	Endocrine hyperfunction		PNA	NGS	PNA-NGS
1	F	Present	Present	Peripheral PP	12.4	R201C	R201C	R201C
2	M	Present	Present	Functional pituitary adenoma*, Functional thyroid adenoma	4.2	R201C	R201C	R201C
3	M	Present	Absent	Cushing syndrome	3.4	R201H	R201H	R201H
4	F	Absent	Present	Peripheral PP	2.9	N.D.	R201C	R201C
5	F	Present	Present	Peripheral PP	1.4	R201H	R201H	R201H
6	M	Present	Present	Absent	0.81	R201H	R201H	R201H
7	M	Present	Present	Cushing syndrome	0.67	R201H	R201H	R201H
8	F	Present	Present	Peripheral PP, Functional thyroid adenoma	0.55	R201H	R201H	R201H
9	M	Present	Present	Functional thyroid adenoma	0.28	R201H	R201H	R201H
10	M	Present	Absent	Pituitary adenoma**	0.26	R201C	R201C	R201C
11	F	Present	Present	Peripheral PP	<0.03	N.D.	N.D.	R201C
12	F	Present	Present	Peripheral PP	<0.03	N.D.	N.D.	R201H
13	F	Absent	Present	Peripheral PP, Functional thyroid adenoma	<0.03	N.D.	N.D.	N.D.
14	F	Present	Absent	Peripheral PP	<0.03	N.D.	N.D.	N.D.
15	F	Present	Absent	Peripheral PP	<0.03	N.D.	N.D.	N.D.
16	F	Present	Present	Absent	<0.03	N.D.	N.D.	N.D.

Abbreviations: FD, osseous fibrous dysplasia; MAS, McCune-Albright syndrome; N.D., not detected; NGS, next generation sequencing; PNA, the peptide nucleic acid method; PNA-NGS, combinatory use of PNA and NGS; PP, precocious puberty.
*Hyperprolactinemia and GH-producing adenoma.
**GH-producing adenoma.
doi:10.1371/journal.pone.0060525.t001

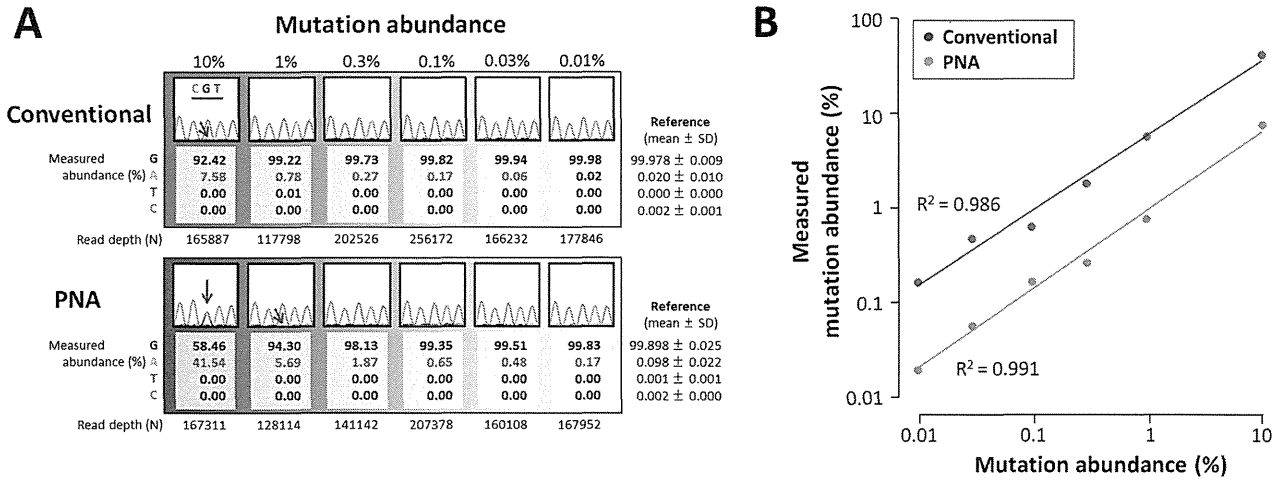

Figure 2. Results of the serial dilution study. **(A)** Cloned mutant DNA (R201H mutation) was diluted into cloned wildtype DNA to 1/10 (10%), 1/100 (1%), 1/333 (0.3%), 1/1,000 (0.1%), 1/3,333 (0.03%) and 1/10,000 (0.01%). Serially diluted DNA samples were PCR-amplified with or without the peptide nucleic acid (PNA) probe ('PNA' and 'Conventional'. Each PCR product was analyzed by Sanger sequencing and next generation sequencing (NGS). Partial chromatograms encompassing the GNAS codon 201 (indicated by CGT) are shown. Relative abundance of the c.602 nucleotide (G, A, T and C) measured by NGS is aligned with each chromatogram. The G allele is wildtype, while the A allele is the R201H mutant. Values with a positive test result (defined by z-score of measured mutant abundance; see Materials and Methods for details) are colored red. Experiment-specific reference ranges are also shown. In the 12 chromatograms, the mutant signal could be detected in two PNA-treated samples and one non-treated sample (indicated by red arrows). Contrastingly, the mutation could be detected down to 0.03% by NGS alone, and down to 0.01% by combinatory use of PNA and NGS. **(B)** A serial dilution plot showing a linear correlation between true mutation abundance and measured mutation abundance. Note that both axes are logarithmic. Comparison of mutation abundance values of PNA-treated and untreated samples revealed that the fold enrichment by PNA is about 7, and it was independent of initial abundance.
doi:10.1371/journal.pone.0060525.g002

Mutation abundance in PBL of MAS patients

To define the distribution of NGS-measured RMA in PBL among MAS patients, we analyzed 16 patient-derived PBL samples. Ten out of 16 genomes had a *GNAS* mutation (R201H, N = 6; R201C, N = 4) of which NGS-measured RMA was more than 0.03% (**Table 1**). NGS-measured RMA ranged from 0.3% to 12.4% (median, 1.1%), which was consistent with the fact that we could not detect those mutations by conventional Sanger sequencing without the PNA probe (data not shown). It is also consistent with the previous genetic knowledge that conventional Sanger sequencing cannot detect *GNAS* mutations in most MAS patient-derived PBL samples [7]. The distributions of NGS-measured RMA were similar between eight patients having all three MAS features and the remaining eight with two features (P = 0.5, Wilcoxon rank sum test).

Comparison of mutation detection methods

Finally, we compared the diagnostic performance of three mutation detection methods: the PNA method, NGS, and combinatory use of PNA and NGS (PNA-NGS). We assessed the detection limits using the serially diluted samples, and found that NGS could detect the mutation down to 0.03%, while the PNA method alone could detect down to 1% (**Figure 2**). The PNA-NGS method had the lowest detection limit, which was 0.01% (**Figure 2**). We also performed a comparative mutation detection study using the 16 patient-derived PBL genome samples. The PNA method identified mutations in nine out of 16 patients (**Table 1**). All of these mutations were also detected by NGS and PNA-NGS. Among seven patients with a negative result by the PNA method, NGS detected one mutation carrier, and PNA-NGS revealed further two mutation carriers (**Table 1**). Collectively, mutation detection rate of PNA, NGS and PNA-NGS was 56%, 63% and 75%, respectively.

Discussion

Detecting low-abundance somatic mutations with next generation amplicon sequencing is becoming a robust analytic tool in cancer genomics. In the present study, we demonstrate that this approach is also effective in diagnosis of a benign disorder due to low-abundance somatic mutations, as shown in megalencephaly syndromes very recently [15].

The quantitative nature of NGS allowed us to investigate the distribution of RMA in patient-derived PBL samples. We showed for the first time that NGS-measured RMA in PBL is strikingly variable among MAS patients. NGS-measured RMA in PBL does not correlate with disease severity, as defined by the number of clinical features, indicating that RMA in PBL and affected lesions are not correlated. Similar results have been observed in syndromes due to activation of AKT signaling (Proteus syndrome [16], and megalencephaly syndromes [15]), thus would be a universal feature of congenital syndromes due to somatic activating mutations.

We verified the diagnostic performance of three mutation detection methods (PNA, NGS and PNA-NGS) using a serial dilution study and a comparative mutation detection study. In both studies, the PNA-NGS method was seemed to be most sensitive. Combination of NGS and PNA resulted in 100-fold decrease in assay detection limit as compared with the PNA method alone. Clearly, this improvement will contribute to more accurate molecular diagnosis of MAS.

In the present study, 56% of MAS patients were positive for a *GNAS* mutation by the PNA method. Similar mutation detection rate with the nested PCR method or the PNA method have been reported [9–11]. Of clinical importance, we could detect *GNAS* mutations by the PNA-NGS method in three out of seven 'PNA-negative' MAS patients. This would be not only due to ultra-deep sequencing of NGS, but also due to nature of the mutation detection methods (qualitative *vs* quantitative), because a patient with relatively high RMA (Patient 4 in **Table 1**) was missed by PNA. Considering that mutation detection rate is more than 90% when affected tissue was available [10], we believe that improvement of mutation detection by the PNA-NGS approach is due to increase of true positives, although we cannot discriminate true positives from false positives in the present study. Future studies using paired PBL-affected tissue(s) samples, which have discordant test results (*e.g.,* negative in PBL but positive in affected tissue(s)) will clarify the true diagnostic performance of the PNA-NGS approach.

In summary, we successfully developed an NGS-based mutation detection method for MAS, allowing quantitative and sensitive molecular diagnosis. The PNA-NGS method achieved 100-fold decrease in assay detection limit, as compared with the PNA method. Our study exemplifies the utility of NGS-based approaches to diagnose congenital disorders due to low-abundance somatic mutations from peripheral blood.

Acknowledgments

We would like to thank the following physicians for sent us clinical samples of MAS patients: Hamajima T (Aichi Children's Health and Medical Center), Hori N (Sanokousei General Hospital), Kamasaki H (Sapporo Medical University School of Medicine), Kamimaki T (Shizuoka City Shimizu Hospital), Kawada Y (Kyushu Rousai Hospital), Motomura K (Nagasaki University), Mukai T (Asahikawa-Kosei General Hospital), Naiki Y (National Center for Child Health and Development), Okada S (Hiroshima University Graduate School of Biomedical Sciences), Suwa T (Gifu University), Tajima T (Hokkaido University School of Medicine), and Tokuhiro E (Odawara Municipal Hospital). We also thank Prof. Takao Takahashi for fruitful discussion.

Author Contributions

Conceived and designed the experiments: SN TH. Performed the experiments: SN KM. Analyzed the data: SN. Contributed reagents/materials/analysis tools: KM TI YT TH. Wrote the paper: SN.

References

1. Ng SB, Turner EH, Robertson PD, Flygare SD, Bigham AW, et al. (2009) Targeted capture and massively parallel sequencing of 12 human exomes. Nature 461: 272–276.
2. Mellmann A, Harmsen D, Cummings CA, Zentz EB, Leopold SR, et al. (2011) Prospective genomic characterization of the German enterohemorrhagic Escherichia coli O104:H4 outbreak by rapid next generation sequencing technology. PLoS One 6: e22751.
3. Thomas RK, Nickerson E, Simons JF, Janne PA, Tengs T, et al. (2006) Sensitive mutation detection in heterogeneous cancer specimens by massively parallel picoliter reactor sequencing. Nat Med 12: 852–855.
4. McCune DJ (1936) Osteitis fibrosa cystica; the case of a nine year old girl who also exhibits precocious puberty, multiple pigmentation of the skin and hyperthyroidism. Am J Dis Child 52: 743–744.
5. Albright F, Butler AM, Hampton AO, Smith P (1937) Syndrome characterized by osteitis fibrosa disseminata, areas of pigmentation and endocrine dysfunction, with precocious puberty in females: report of five cases. N Engl J Med 216: 727–746.
6. Weinstein LS, Shenker A, Gejman PV, Merino MJ, Friedman E, et al. (1991) Activating mutations of the stimulatory G protein in the McCune-Albright syndrome. N Engl J Med 325: 1688–1695.

7. Candeliere GA, Roughley PJ, Glorieux FH (1997) Polymerase chain reaction-based technique for the selective enrichment and analysis of mosaic arg201 mutations in G alpha s from patients with fibrous dysplasia of bone. Bone 21: 201–206.
8. Bianco P, Riminucci M, Majolagbe A, Kuznetsov SA, Collins MT, et al. (2000) Mutations of the GNAS1 gene, stromal cell dysfunction, and osteomalacic changes in non-McCune-Albright fibrous dysplasia of bone. J Bone Miner Res 15: 120–128.
9. Hannon TS, Noonan K, Steinmetz R, Eugster EA, Levine MA, et al. (2003) Is McCune-Albright syndrome overlooked in subjects with fibrous dysplasia of bone? J Pediatr 142: 532–538.
10. Lumbroso S, Paris F, Sultan C, European Collaborative S (2004) Activating Gsalpha mutations: analysis of 113 patients with signs of McCune-Albright syndrome--a European Collaborative Study. J Clin Endocrinol Metab 89: 2107–2113.
11. Kalfa N, Philibert P, Audran F, Ecochard A, Hannon T, et al. (2006) Searching for somatic mutations in McCune-Albright syndrome: a comparative study of the peptidic nucleic acid versus the nested PCR method based on 148 DNA samples. Eur J Endocrinol 155: 839–843.
12. Langmead B, Trapnell C, Pop M, Salzberg SL (2009) Ultrafast and memory-efficient alignment of short DNA sequences to the human genome. Genome Biol 10: R25.
13. Li H, Handsaker B, Wysoker A, Fennell T, Ruan J, et al. (2009) The Sequence Alignment/Map format and SAMtools. Bioinformatics 25: 2078–2079.
14. Lee SE, Lee EH, Park H, Sung JY, Lee HW, et al. (2012) The diagnostic utility of the GNAS mutation in patients with fibrous dysplasia: meta-analysis of 168 sporadic cases. Hum Pathol 43: 1234–1242.
15. Riviere JB, Mirzaa GM, O'Roak BJ, Beddaoui M, Alcantara D, et al. (2012) De novo germline and postzygotic mutations in AKT3, PIK3R2 and PIK3CA cause a spectrum of related megalencephaly syndromes. Nat Genet 44: 934–940.
16. Lindhurst MJ, Sapp JC, Teer JK, Johnston JJ, Finn EM, et al. (2011) A mosaic activating mutation in AKT1 associated with the Proteus syndrome. N Engl J Med 365: 611–619.

Atsuko Yoshizawa-Ogasawara*, Sayaka Ogikubo, Mari Satoh, Satoshi Narumi and Tomonobu Hasegawa

Congenital hypothyroidism caused by a novel mutation of the dual oxidase 2 *(DUOX2)* gene

Abstract: The dual oxidase 2 *(DUOX2)* mutation results in an impairment of the hydrogen peroxidase-generating system and is identified as a dyshormonogenic cause of congenital hypothyroidism (CH). Here, we describe two unrelated Japanese girls with CH due to a novel *DUOX2* mutation. They had high serum thyrotropin levels and low free thyroxine/thyroxine concentrations during the neonatal period. A novel missense mutation with a transversion of G to A at position 1462 in exon 12 of the *DUOX2* gene that caused a replacement of glycine (G) with arginine (R) at codon 488 of the protein (c.1462G>A, p.[G488R]) was identified. One patient was a compound heterozygote for p.[L479SfsX3]+[G488R]. The other was homozygous for p.[G488R]. This p.G488R substitution occurred in a highly conserved glycine residue of the mammalian DUOX2 protein. The two patients had different haplotypes, suggesting that the p.G488R alleles were the result of independent, recurrent mutations. Later in life, both patients were still euthyroid even after discontinuing thyroid hormone therapy. We conclude that this p.G488R missense mutation in the *DUOX2* gene of the patients is associated with thyroid dysfunction that presents during the neonatal period.

Keywords: congenital hypothyroidism; dual oxidase 2 *(DUOX2)*; dyshormonogenesis; G488R mutation; neonatal screening.

***Corresponding author: Atsuko Yoshizawa-Ogasawara,** Okinaka Memorial Institute for Medical Research, 2-2-2 Toranomon, Minato-ku, Tokyo 105-8470, Japan,
E-mail: ayoshizawa-endo@umin.ac.jp
Atsuko Yoshizawa-Ogasawara: Department of Pediatrics, Ibaraki Children's Hospital, Mito, Japan
Sayaka Ogikubo: Okinaka Memorial Institute for Medical Research, Tokyo, Japan
Mari Satoh: Department of Pediatrics, Toho University Omori Medical Center, Tokyo, Japan
Satoshi Narumi and Tomonobu Hasegawa: Department of Pediatrics, Keio University School of Medicine, Tokyo, Japan

Introduction

Congenital hypothyroidism (CH) occurs with an incidence of 1 in 4000 worldwide (1), while the incidence of CH in Japan currently ranges from 1 in 2200 to 1 in 2500 births (2). Neonatal screening programs for CH allow for early diagnosis and treatment. Lowering the bloodspot-thyrotropin (TSH) threshold to 10 mU/L has increased the ability of neonatal screening programs to detect hyperthyrotropinemia, which is characterized by elevated TSH levels and normal thyroxine (T_4) (2). The most common cause of CH, which accounts for up to 75%–80% of cases, is thyroid dysgenesis caused by aplasia, hypoplasia, or ectopic thyroid (3). Dyshormonogenesis accounts for the remaining 15%–20% of CH cases (3). Lifelong thyroid hormone replacement is usually required in cases of thyroid dyshormonogenesis. However, some patients can discontinue their medication after a period of replacement therapy.

Recent data from a study conducted in Italy (4) have shown that the percentage of defects associated with thyroid gland in situ cases has increased to 68%, and thyroid dysgenesis accounted for 32% of the CH cases with a bloodspot-TSH threshold of 12 or 10 mU/L. In a report from Japan, thyroid dysgenesis accounted for 63.2% of cases and dyshormonogenesis accounted for 36.8% of cases identified between 1981 and 1988 (2).

The recently identified gene mutations associated with CH that result in dyshormonogenesis involve dual oxidases (DUOXs), thyroid peroxidase (TPO), thyroglobulin (TG), sodium iodide symporter (NIS), pendrin (PDS) (1, 5), dual oxidase maturation factor 2 (DUOXA2) (6), and dehalogenase 1 (DEHAL1) (7). Biallelic mutations in the *TPO* gene can lead to total iodide organification defect (TIOD) when the resulting enzymatic impairment is severe (8–10). It has also been reported that some patients with TPO mutations exhibit partial iodide organification defect (PIOD) (10). Other candidate genes in which mutations lead to PIOD include *DUOX2* and *PDS*. Biallelic homozygous or compound heterozygous *DUOX2* mutations lead to goitrous CH (11–13), whereas monoallelic non-sense mutations cause transient CH (11, 14).

Here, we describe a novel p.G488R mutation in the *DUOX2* gene, identified in two unrelated Japanese patients with CH during a neonatal screening. One patient had a compound heterozygous mutation (p.[L479SfsX3]+[G488R]), while the other had a homozygous mutation (p.[G488R]+[G488R]); however, both were able to discontinue thyroid hormone therapy.

Patients and methods

Patients

Two patients from unrelated families were studied. These families were from different regions of Japan, and neither of the subjects had a family history of thyroid disease. The daily iodine intake (500–1000 μg) of the two patients and their mothers conformed to the nutritional standards of Japan, which averages 500–1500 μg/day (15, 16). Blood samples for the neonatal CH screening were collected within 5 days after birth. TSH levels were measured using blood filter papers. In cases where the TSH level was >10 mU/L, further examinations were performed. For the assessment of the permanence of hypothyroidism, L-T_4 administration is discontinued for 30 days at some point after the child reaches 3 years of age if no permanent cause of CH was found by scan or there was no TSH increase after the newborn period, as recommended by the American Academy of Pediatrics (AAP) (17). In more severely affected children, thyroid hormone replacement dosage is reduced by half. If the serum TSH value has not increased, then thyroid hormone treatment is discontinued for another 30 days with repeated serum free T_4 (fT_4) and TSH determination (17). In these two patients, thyroid function was reevaluated as per the AAP recommendation. Because perchlorate is not available for medical use in Japan, no perchlorate discharge test could be performed.

Patient 1, a child of a non-consanguineous couple, was delivered without complications after 38 weeks of gestation. Her TSH and fT_4 levels were 56.98 mU/L and 0.54 ng/dL, respectively, during the neonatal screening. During her first hospital visit, the patient's TSH level was 64.5 mU/L and her T_4 level was 4.5 μg/dL (Table 1). The core size of the patient's distal femur was 6 mm according to her X-ray. She received levothyroxine (L-T_4) supplementation (initial dose of 10 μg/kg/day). The patient's TSH level at neonatal screening was >50 mU/L, and a replacement dose of 3 μg/kg/day (45 μg/day) L-T_4 was still required when she was 3 years old owing to increased TSH levels. Therefore, a reassessment was performed after she entered elementary school. Because the replacement dose of L-T_4 was lowered to 1 μg/kg/day (25 μg/day) when she was 8 years old, L-T_4 treatment was discontinued for 30 days with repeated serum fT_4 and TSH determination. A soft, small thyroid was palpable for 3 years after she stopped taking the medication. The total volume of her thyroid gland was calculated as the sum of each lobe according to ultrasonography and measured 3.08 cm^3, a normal volume compared with that derived from healthy children with the same body height [mean (SD), 4.9 (1.1) cm^3]. A perchlorate discharge test was not performed. Her motor and mental development and her hearing were all normal. Her height and weight were 164 cm (+1.5 SD) and 61 kg (+1.4 SD), respectively, at 15 years of age, and her pubertal development was normal. Currently, her thyroid gland is not enlarged. The total volume of her thyroid gland is 12.1 cm^3 [mean (SD), 10.9 (2.5) cm^3] as measured by ultrasonography. She is still euthyroid (Table 1), and her urinary iodine level is 422 μg/L (Table 1). She attends high school and has no educational problems. Her mother has TSH and fT_4 levels of 1.37 mU/L and 0.98 ng/dL, respectively, at 49 years of age. Her father, at 52 years of age, has TSH and fT_4 levels of 0.727 mU/L and 1.00 ng/dL, respectively (Table 1).

Patient 2, the first child of a non-consanguineous couple, was delivered without complications after 40 weeks and 5 days of gestation. The patient's TSH level during the neonatal screening was >50 mU/L. During her first hospital visit, the patient's TSH and fT_4 levels were 165 mU/L and 0.3 ng/dL, respectively (Table 1). The patient's TG level then increased to 2350 ng/mL. The core size of her distal femur was 6 mm as measured by X-ray. L-T_4 treatment was initiated (10 μg/kg/day), and the patient's TG level decreased to 23.6 ng/mL 3 months later. Ultrasonography images indicated that her thyroid gland was in the proper location with a total volume of 1.7 cm^3 [mean (SD), 2.3 (0.7) cm^3]. The patient's motor and mental development and her hearing were all normal. Her TSH level was 165 mU/L at her first hospital visit, and the replacement dose of L-T_4 was still required at >5 μg/kg/day (70 μg/day) because of increased TSH at 3 years of age. Therefore, an attempt was made to discontinue the medication when she was 6 years old. However, she still required further replacement therapy because of her increased TSH level. After her replacement dose was lowered to 0.75 μg/kg/day (25 μg/day), L-T_4 treatment was then discontinued at 12 years of age. A perchlorate discharge test was not performed, and urinary iodine was not examined. At 12 years of age, her height and weight were 145 cm (−0.2 SD) and 35 kg (−0.2 SD), respectively. She is currently euthyroid (Table 1). She attends junior high school and has no educational problems. Her pubertal development is normal, and her younger brother tested negative for CH during his neonatal screening. Her mother, who is in her 30 s, has TSH and fT_4 levels of 1.57 mU/L and 1.07 ng/dL, respectively (Table 1). It is currently not possible to study thyroid function and gene analysis in other family members.

Laboratory tests

TSH levels were measured using an electrochemiluminescence immunoassay (ECLIA) (Architect; Abbott, Wiesbaden, Germany), with a reference range of 0.50–5.00 mU/L. FT_4 (0.90–1.70 ng/dL) (Architect, Abbott), T_4 (6.10–12.4 μg/dL) (Elecsys T_4 II; Roche Diagnostics, Mannheim, Germany), and TG (<6 months old, <95 ng/mL; >6 months old, <32.7 ng/mL) (Elecsys Tg, Roche Diagnostics) levels were also measured using an ECLIA. According to X-rays, the core size of the distal femur was measured, with a reference range of 4.1 to 9.7 mm for babies born after 37 weeks of gestation (18). The total volume of the thyroid gland was calculated using ultrasonography, with a reference range derived from healthy children with the same body height (19). The concentration of urinary iodine was measured using colorimetry (median 262 μg/L) (Iodine Monit; Hitachi Chemical, Tokyo, Japan).

DNA sequence analysis

Genomic DNA was isolated from peripheral blood lymphocytes. All exons of the *DUOX2* gene were amplified by polymerase chain reaction (PCR) using primers described in previous studies (11). The

	Reference values	Patient 1	Patient 2
Sex		Female	Female
Family history		–	–
Deafness		–	–
Neonatal screening			
Age, day		5	5
TSH, mU/L	<10	56.98	>50
fT_4, ng/dL	0.90–1.70	0.54	NA
First visit			
Age		1 month	13 days
TSH, mU/L	0.50–5.00	64.5	165
fT_4, ng/dL	0.90–1.70	NA	0.3
T_4, µg/dL	6.10–12.4	4.5	1.8
Recent data			
Age, years		17	14
TSH, mU/L	0.50–5.00	2.33	4.32
fT_4, ng/dL	0.90–1.70	0.95	1.10
TG, ng/mL	<32.7	57.1	37.2
L-T_4 therapy		–	–
Age at T_4 withdrawal, years		8	12
Urinary iodine, µg/L	Median, 262	422	NA
Gene, Genotype		*DUOX2*, p.[L479SfsX3]+[G488R]	*DUOX2*, p.[G488R]+[G488R]
Mother			
Age, years		49	30s
TSH, mU/L	0.50–5.00	1.37	1.57
fT_4, ng/dL	0.90–1.70	0.98	1.07
Gene, Genotype		*DUOX2*, p.[L479SfsX3]	*DUOX2*, p.[G488R]
Father			
Age, years		52	NA
TSH, mU/L	0.50–5.00	0.72	NA
fT_4, ng/dL	0.90–1.70	1.00	NA
Gene, Genotype		*DUOX2*, p.[G488R]	NA

Table 1 Clinical, biochemical, and genetic data.
TSH, thyrotropin; fT_4, free thyroxine; T_4, thyroxine; TG, thyroglobulin; L-T_4, levothyroxine; NA, not available.

purified PCR products were directly sequenced using an automated DNA sequence analyzer (ABI 3130*xl*; Applied Biosystems, Foster City, CA, USA). The PCR products containing *DUOX2* mutations were subcloned to pCR2.1 vectors using a TA-cloning kit (Invitrogen, San Diego, CA, USA) to determine the specific changes in the nucleotide sequence. Transformation of the products was performed according to the manufacturer's instructions. As for patients harboring mutations in DUOX2, we also sequenced the other genes implicated in CH, including *TSHR*, *PAX8*, *NKX2.1*, *NKX2.5*, *FOXE1*, *TPO*, *TG*, *NIS*, *PDS*, *DUOXA2*, and *DEHAL1* using the MiSeq instrument (Illumina Inc., San Diego, CA, USA) according to the SureSelect protocol (Agilent Technologies, Santa Clara, CA, USA). Briefly, 3 µg of genomic DNA was used for the SureSelect capture method. Exons of the 97 known genes associated with congenital endocrine disorders (including 11 CH-related genes) were identified in the University of California Santa Cruz table browser (http://genome.ucsc.edu/). In total, we targeted 902 regions comprising 200,675 bp using the SureSelect method. DNA obtained from SureSelect solution-based sequence capture was subjected to MiSeq sequencing according to the manufacturer's protocol. This study was approved by the Ethics Committees at Ibaraki Children's Hospital, Toho University, and Okinaka Memorial Institute for Medical Research. Written informed consent was obtained from the parents of the subjects.

Results

Molecular analysis

Direct sequencing of the genomic DNA revealed that patient 1 had a biallelic compound heterozygous mutation in the *DUOX2* gene. One was a novel missense mutation with a transversion of G to A at 1462 in exon 12 that replaced glycine (G) with arginine (R) at codon 488 (c.1462G>A, p.[G488R]) (Figure 1A). The other mutation was a deletion-insertion mutation in exon 12 of the *DUOX2* gene where AG replaced the nucleotide sequence of CTATCC at base pairs 1435–1440. This deletion-insertion

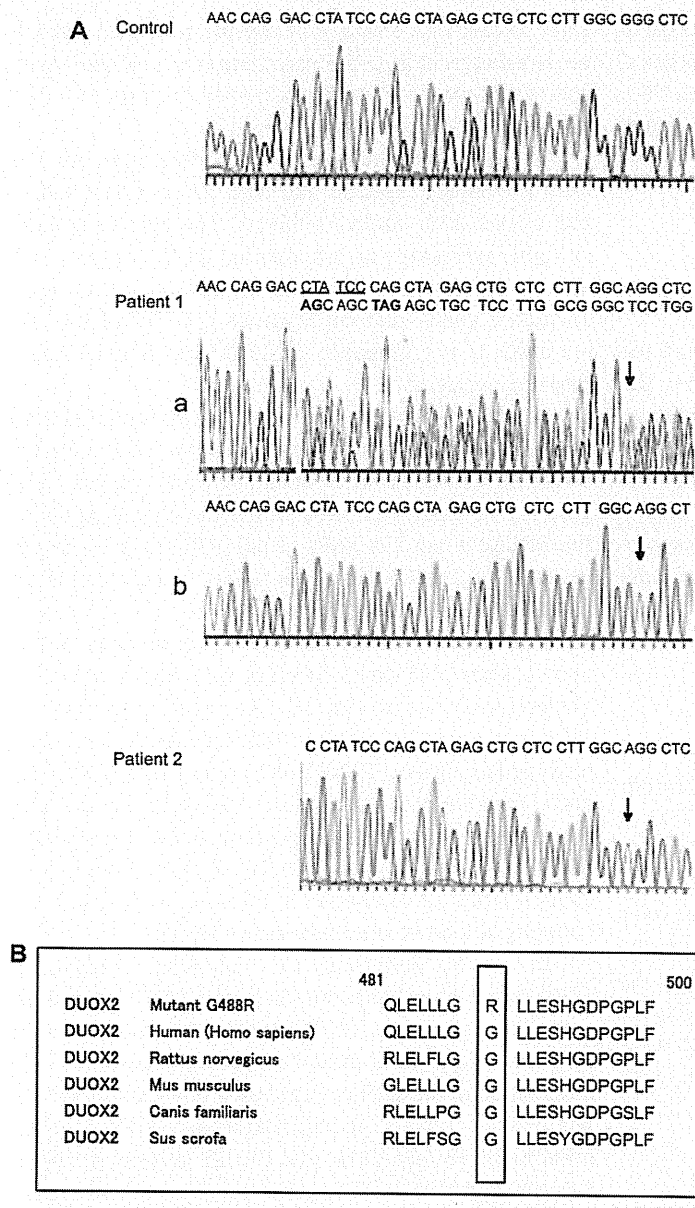

Figure 1 (A) Sequencing chromatograms of DUOX2 exon 12 from a control subject, patient 1, and patient 2. The arrows indicate the position of the monoallelic or biallelic G to A mutation (c.1462G>A). Patient 1 is heterozygous for a deletion of CTATCC (underlined) and an insertion of AG (bold) at position 1435–1440. The deletion-insertion leads to a frameshift producing a stop codon at amino acid 481 (bold) (a). In one allele, the sequence after TA cloning indicates a transversion of G to A at position 1462, resulting in a monoallelic p.G488R mutation (b). Patient 2 has a biallelic G to A mutation. (B) Analysis of DUOX2 protein homology among different species. The glycine residue mutated to arginine (p.G488R) in the patients is highly conserved in mammalian DUOX2 proteins.

leads to a frameshift producing a stop at codon 481 (c.1435_1440delCTATCCinsAG, p.[L479SfsX3]) (Figure 1A). The unaffected mother of patient 1 had a monoallelic mutation p.[L479SfsX3], and the unaffected father of patient 1 had a monoallelic mutation p.[G488R] (Table 1).

Patient 2 had a biallelic mutation p.[G488R]+[G488R] in the *DOUX2* gene (Figure 1A). After obtaining written informed consent, a gene analysis of the mother of patient 2 was performed and a monoallelic mutation p.[G488R] was identified in the *DUOX2* gene (Table 1).

This novel p.G488R substitution occurred in a highly conserved glycine residue of the mammalian DUOX2 protein (Figure 1B) and was not detected in the 100 alleles analyzed from 50 additional control subjects. The

deletion-insertion mutation p.[L479SfsX3] was reported in 2008 (20). Neither one of the patients had any additional mutations of TSHR, PAX8, NKX2.1, NKX2.5, FOXE1, TPO, TG, NIS, PDS, DUOXA2, or DEHAL1 except for a previously reported TG polymorphism (Reference SNP Cluster Report: rs2076737).

Founder effect

We identified two unrelated patients who also had the novel p.G488R mutation. To distinguish whether the recurrent p.G488R alleles were derived from a common ancestral allele or occurred independently, we analyzed 12 single nucleotide polymorphisms (SNPs) within the coding region of the *DUOX2* gene (Table 2). The patients with the p.G488R mutation had different haplotypes, suggesting that the p.G488R alleles were the result of independently occurring mutations.

Discussion

The mutated CH genes resulted in defective thyroid hormone synthesis that has recently been identified to include the *DUOXs*, *TPO*, *TG*, *NIS*, *PDS* (1, 5), *DUOXA2* (6), and *DEHAL1* (7) genes. A decrease in hydrogen peroxidase (H_2O_2) generation due to *DUOX2* gene mutations has been recognized as one cause of thyroid dyshormonogenesis (11). Other cases of CH caused by *DUOX2* gene mutations in infants have also been identified (12–14). In Japan, novel mutations in the *DUOX2* gene were detected in eight Japanese patients with transient CH (20) and one Japanese adult patient with a dyshormonogenic goiter (21). Moreover, Grasberger et al. (22), Tonacchera et al. (23), and Hoste et al. (24) have also recently published functional studies of novel DUOX2 mutations.

Exon	cDNA	Nucleotide	Frequency in control subjects	G488R	
				Patient 1	Patient 2
3	303	C, A	95; 5	CC	CC
4	413	C, T	11; 89	TT	TT
5	558	C, T	48; 52	CT	CT
	567	C, T	46; 54	CT	TT
	597	G, C	46; 54	GC	GC
	598	G, A	46; 54	GA	GA
	633	C, T	46; 54	CT	CT
12	1461	G, C	4; 96	CC	CC
16	2033	A, G	93; 7	AA	AA
24	3200	C, T	15; 85	TT	TT
29	3966	C, T	96; 4	CC	CC
32	4479	C, G	95; 5	CC	CC

Table 2 Twelve SNPs in patients with G488R mutation.

The p.G488R mutation in the *DUOX2* gene has not been previously reported and was also not detected in 100 alleles from control subjects. The glycine residue is highly conserved in mammalian *DUOX2* genes, and neither patient had additional mutations in the other candidate genes that could cause CH. Therefore, this mutation is the probable cause of hypothyroidism in these two patients.

To evaluate whether this mutation was inherited from a common ancestral chromosome or an independently occurring mutation in a heterogeneous genetic background, we studied 12 SNPs within the coding region of the *DOUX2* gene. The SNPs of p.G488R alleles were not identical, suggesting that the p.G488R mutation is an independently occurring mutation.

The *DUOX2* gene is localized to chromosome 15q15.3 and consists of 33 exons encoding an mRNA that is 6376 nucleotides in length (25, 26). The encoded protein is a 1548-amino-acid polypeptide that includes a 26-amino-acid signal peptide. The DUOX2 protein localizes to the apical membrane of thyrocytes and is involved in the Ca^{2+}/reduced nicotinamide adenine dinucleotide phosphate-dependent generation of H_2O_2 (27). TPO requires H_2O_2 to catalyze both the iodination of tyrosine residues and the coupling of iodotyrosine residues on TG (28).

In reports describing the functional analysis of *DUOX2* gene mutations, the Q36H and R376W mutations completely abolished DUOX2 function (22). The D506N mutation displayed a partial deficiency phenotype with a reduction in the surface expression of a mutant protein with normal intrinsic activity that is involved in the generation of H_2O_2 (22). S911L and C1052Y mutations caused a partial defect in the H_2O_2-generating system and caused reduced expression of DUOX2 at the cell surface (23). Moreover, the G1518S mutation abolished protein activity despite expression at the cell surface (24). G488R localizes to the extracellular region of DUOX2, which contains a TPO-like domain. This suggests that the G488R mutation likely results in a partial impairment of function, although the expression of the mutant protein has not yet been studied.

Previously, Varela et al. (13) and Chiesa et al. (29) reported *DUOX2* gene mutations in three Argentinean patients with CH. One patient was a compound heterozygote for p.[Q36H]+[S965fsX994], and his perchlorate discharge test result (46%) at 5 years of age (reference value, <10%) indicated PIOD. Two siblings in another family who were

compound heterozygotes for p.[G418fsX482]+[skipping of exon 20] also presented with PIOD (a female with a 68% perchlorate discharge at 4.5 years, and her younger brother with 60% at 4 years). In another report (12), two siblings in an Italian family were compound heterozygotes for p.[R376W]+[R842X]. Their discharge rates after perchlorate administration were 28% in the older boy at 4 years of age and 12% in his younger brother at 4 years of age (reference value, 0%). In this study, no perchlorate discharge test could be performed; however, the patients harboring a compound heterozygous mutation for p.[L479SfsX3]+[G488R] or a homozygous mutation for p.[G488R] would be unlikely to represent TIOD.

Maruo et al. (20) reported that transient CH was diagnosed in eight Japanese patients with biallelic mutations in the *DUOX2* gene. Four patients had transient, but not permanent CH, caused by a compound heterozygous mutation for p.[L479SfsX3]+[K628RfsX11] that completely inactivated DUOX2. This suggested that the need for thyroid hormone decreased after the neonatal period, and the activity of DUOX1-dependent oxidases in thyrocytes became sufficient for adequate thyroid hormone synthesis.

Our study involved two Japanese patients in whom CH was diagnosed during a neonatal screening. These patients had either a compound heterozygous or a homozygous p.G488R mutation but had no mutations in the other candidate genes that would be expected to lead to CH. These patients required thyroid hormone replacement therapy, which was initiated during the neonatal period. After the thyroid function improved, L-T_4 replacement therapy was discontinued in both patient 1 (at 8 years of age) and patient 2 (at 12 years of age). The father of patient 1 and the mother of patient 2 were heterozygous for this missense mutation but exhibited no obvious thyroid dysfunction. Indeed, the absence of functional characterization of the G488R mutation associated with CH could not explain the DUOX2 phenotype. Nonetheless, their clinical, biochemical, and genetic data strongly indicate that a novel G488R mutation of the *DUOX2* gene caused their dyshormonogenesis. From these observations, we therefore hypothesize that the biallelic mutation of the *DUOX2* gene in these cases causes a mild decrease in thyroid function. It is still unclear why these cases were mild, whereas other cases involving biallelic mutations of the *DUOX2* gene cause permanent hypothyroidism. We propose the following as possible explanations for this discrepancy: First, Japan is considered to be an iodine-sufficient area because of the ingestion of large quantities of iodine-rich seaweed (30). Iodide plays an important role in the control of H_2O_2 production, regulating DUOX activity in a dual fashion, where it is stimulatory at low concentrations and inhibitory at high concentrations (31–33). In the absence of iodide, the H_2O_2 produced by DUOX2 decreases the activity of both TPO and DUOX (34). Second, the DUOX1 enzyme is able to generate extracellular H_2O_2 in thyroid cells, suggesting that DUOX1 could partially compensate for the loss of DUOX2 (35). Third, Hulur et al. (36) have recently reported a case in which a patient heterozygous for p.[C189R] within DUOXA2 lacks one allele of DUOX2, DUOXA2, and DUOXA1 but has two functioning DUOX1 alleles and presents with mild and transient CH. This suggests that DUOX1 could play a role in H_2O_2 production. Therefore, it is conceivable that, with sufficient iodine intake, the H_2O_2 provided by DUOXs might be sufficient to maintain thyroid function after the neonatal period in some Japanese patients. Furthermore, the phenotype might depend not only on DUOX2 alone but also on other factors that are involved in the generation of H_2O_2 by DUOX2.

In conclusion, we describe two patients with CH that have a novel p.G488R mutation in the *DUOX2* gene. The compound heterozygous or homozygous p.G488R mutation resulted in CH that presented during the neonatal period as low T_4 and high TSH levels, resulting in elevated TG. L-T_4 replacement was initiated during the neonatal period and was discontinued in both patients, who are currently euthyroid.

Acknowledgments: We would like to thank Dr. Shohei Harada (Tokyo, Japan) and Dr. Akira Hishinuma (Tochigi, Japan) for their helpful suggestions about the preparation of our manuscript. This work was supported in part by the Health Science Research Grant for Research on Applying Health Technology [Jitsuyoka (Nanbyo)-Ippan-014] from the Ministry of Health, Labour and Welfare of Japan (SN, TH).

Conflict of interest statement

Disclosure Summary: The authors have nothing to disclose.

Received March 20, 2012; accepted October 5, 2012

References

1. Knobel M, Medeiros-Neto G. An outline of inherited disorders of the thyroid hormone generating system. Thyroid 2003;13:771–801.

2. Harada S. Incidence and etiology of permanent congenital hypothyroidism (cretinism). Horm Rinsho 2007;55:537–43.

3. De Felice M, Di Lauro R. Thyroid development and its disorders: genetics and molecular mechanisms. Endocr Rev 2004;25: 722–46.
4. Corbetta C, Weber G, Cortinovis F, Calebiro D, Passoni A, et al. A 7-year experience with low blood TSH cutoff levels for neonatal screening reveals an unsuspected frequency of congenital hypothyroidism (CH). Clin Endcrinol (Oxf) 2009;71:739–45.
5. Park SM, Chatterjee VK. Genetics of congenital hypothyroidism. J Med Genet 2005;42:379–89.
6. Zamproni I, Grasberger H, Cortinovis F, Vigone MC, Chiumello G, et al. Biallelic inactivation of the dual oxidase maturation factor 2 (DUOXA2) gene as a novel cause of congenital hypothyroidism. J Clin Endocrinol Metab 2008;93:605–10.
7. Moreno JC, Klootwijk W, Toor H, Pinto G, D'Alessandro M, et al. Mutations in the iodotyrosine deiodinase gene and hypothyroidism. N Engl J Med 2008;358:1811–8.
8. Bikker H, Vulsma T, Baas F, de Vijlder JJ. Identification of five novel inactivating mutations in the human thyroid peroxidase gene by denaturing gradient gel electrophoresis. Hum Mutat 1995;6:9–16.
9. De Vijlder JJ. Primary congenital hypothyroidsm: defects in iodine pathways. Eur J Endocrinol 2003;149:247–56.
10. Ris-Stalpers C, Bikker H. Genetics and phenomics of hypothyroidism and goiter due to TPO mutations. Mol Cell Endocrinol 2010;322:38–43.
11. Moreno JC, Bikker H, Kempers MJ, van Trotsenburg AS, Baas F, et al. Inactivating mutations in the gene for thyroid oxidase 2 (THOX2) and congenital hypothyroidism. N Engl J Med 2002;347:95–102.
12. Vigone MC, Fugazzola L, Zamproni I, Passoni A, Di Candia S, et al. Persistent mild hypothyroidism associated with novel sequence variants of the DUOX2 gene in two siblings. Hum Mutat 2005;26:395.
13. Varela V, Rivolta CM, Esperante SA, Gruñeiro-Papendieck L, Chiesa A, et al. Three mutations (p.Q36H, p.G418fsX482, and g.IVS19-2A>C) in the dual oxidase 2 gene responsible for congenital goiter and iodide organification defect. Clin Chem 2006;52:182–91.
14. Pfarr N, Korsch E, Kaspers S, Herbst A, Stach A, et al. Congenital hypothyroidism caused by new mutations in the thyroid oxidase 2 (THOX2) gene. Clin Endocrinol (Oxf) 2006;65:810–5.
15. Suzuki H, Higuchi T, Sawa K, Ohtaki S, Horiuchi Y. Endemic coast goiter in Hokkaido, Japan. Acta Endocrinol (Copenh) 1965;50:161–4.
16. Katamine S, Mamiya Y, Sekimoto K, Hoshino N, Totsuka K, et al. Iodine content of various meals currently consumed by urban Japanese. J Nutr Sci Vitaminol 1986;32:487–95.
17. American Academy of Pediatrics, Rose SR, Section on Endocrinology and Committee on Genetics, American Thyroid Association, Brown RS, et al. Update of newborn screening and therapy for congenital hypothyroidism. Pediatrics 2006;117:2290–303.
18. Mahony BS, Callen PW, Filly RA. The distal femoral epiphyseal ossification center in the assessment of third-trimester menstrual age: sonographic identification and measurement. Radiology 1985;155:201–4.
19. Ueda D. Normal volume of the thyroid gland in children. J Clin Ultrasound 1990;18:455–62.
20. Maruo Y, Takahashi H, Soeda I, Nishikura N, Matsui K, et al. Transient congenital hypothyroidism caused by biallelic mutations of the dual oxidase 2 gene in Japanese patients detected by a neonatal screening program. J Clin Endocrinol Metab 2008;93:4261–7.
21. Ohye H, Fukata S, Hishinuma A, Kudo T, Nishihara E, et al. A novel homozygous missense mutation of the dual oxidase 2 (DUOX2) gene in an adult patient with large goiter. Thyroid 2008;18:561–6.
22. Grasberger H, De Deken X, Miot F, Pohlenz J, Refetoff S. Missense mutations of dual oxidase 2 (DUOX2) implicated in congenital hypothyroidism have impaired trafficking in cells reconstituted with DUOX2 maturation factor. Mol Endocrinol 2007;21:1408–21.
23. Tonacchera M, De Marco G, Agretti P, Montanelli L, Di Cosmo C, et al. Identification and functional studies of two new dual-oxidase 2 (DUOX2) mutations in a child with congenital hypothyroidism and a eutopic normal-size thyroid gland. J Clin Endocrinol Metab 2009;94:4309–14.
24. Hoste C, Rigutto S, Van Vliet G, Miot F, De Deken X. Compound heterozygosity for a novel hemizygous missense mutation and a partial deletion affecting the catalytic core of the H_2O_2-generating enzyme DUOX2 associated with transient congenital hypothyroidism. Hum Mutat 2010;31:E1304–18.
25. Dupuy C, Ohayon R, Valent A, Neol-Hudson MS, Deme D, et al. Purification of a novel flavoprotein involved in the thyroid NADPH oxidase. J Biol Chem 1999;274:37265–9.
26. De Deken X, Wang D, Many MC, Costagliola S, Libert F, et al. Cloning of two human thyroid cDNAs encoding new members of the NADPH oxidase family. J Biol Chem 2000;275:23227–33.
27. Caillau B, Dupuy C, Lacroix L, Nocera M, Talbot M, et al. Expression of reduced nicotinamide adenine dinucleotide phosphate oxidase (ThoX, LNOX, Duox) genes and proteins in human thyroid tissues. J Clin Endocrinol Metab 2001;86:3351–8.
28. Corvilain B, Van Sande J, Laurent E, Dumont JE. The H_2O_2-generating system modulates protein iodination and the activity of the pentose phosphate pathway in dog. Endocrinology 1991;128:779–85.
29. Chiesa A, Rivolta CM, Targovnik HM, Gruñeiro-Papendieck L. Clinical, biochemical, and molecular findings in Argentinean patients with goitrous congenital hypothyroidism. Endocrine 2010;38:377–85.
30. Tajiri J, Higashi K, Morita M, Umeda T, Sato T. Studies of hypothyroidism in patients with high iodine intake. J Clin Endocrinol Metab 1986;63:412–7.
31. Corvilain B, Collyn L, Van Sande J, Dumont JE. Stimulation by iodide of H_2O_2 generation in thyroid slices from several species. Am J Physiol Endocrinol Metab 2000;278:E692–9.
32. Cardoso LC, Martin DC, Figueiredo MD, Rosenthal D, Vaisman M, et al. Ca(2+)/nicotinamide adenine dinucleotide phosphate-dependent H_2O_2 generation is inhibited by iodide in human thyroids. J Clin Endocrinol Metab 2001;86:4339–43.
33. Morand S, Chaaraoui M, Kaniewski J, Dème D, Ohayon R, et al. Effect of iodide on nicotinamide adenine dinucleotide phosphate oxidase activity and Duox2 protein expression in isolated porcine thyroid follicles. Endocrinology 2003;144:1241–8.
34. Fortunato RS, Lima de Souza EC, Ameziane-el Hassani R, Boufraqech M, Weyemi U, et al. Functional consequences of dual oxidase-thyroperoxidase interaction at the plasma membrane. J Clin Endocrinol Metab 2010;95:5403–11.

35. Rigutto S, Hoste C, Grasberger H, Milenkovic M, Communi D, et al. Activation of dual oxidases Duox1 and Duox2. J Biol Chem 2009;284:6725–34.
36. Hulur I, Hermanns P, Nestoris C, Heger S, Refetoff S, et al. A single copy of the recently identified dual oxidase maturation factor *(DUOXA)* 1 gene produces only mild transient hypothyroidism in a patient with a novel biallelic DUOXA2 mutation and monoallelic DUOXA1 deletion. J Clin Endocrinol Metab 2011;96: E841–5.

THYROID
Volume 22, Number 10, 2012

DOI: 10.1089/thy.2011.0450

CASE STUDY

Long-Term 3,5,3′-Triiodothyroacetic Acid Therapy in a Child with Hyperthyroidism Caused by Thyroid Hormone Resistance: Pharmacological Study and Therapeutic Recommendations

Rie Anzai,[1] Masanori Adachi,[1] Noriko Sho,[2] Koji Muroya,[1] Yumi Asakura,[1] and Kazumichi Onigata[3]

Background: The effectiveness of short-term 3,5,3′-triiodothyroacetic acid (TRIAC) therapy for the treatment of hyperthyroidism caused by thyroid hormone resistance (RTH) has been documented. Here, we report a 3-year course of TRIAC therapy in an RTH boy, with a quantitative evaluation of the therapeutic effects and pharmacological study of TRIAC.
Patient findings: The gene encoding the thyroid hormone receptor beta (*THRB*) of the patient carries a P453T mutation. During treatment with up to 3.0 mg TRIAC per day, reduction in the thyroid volume, resolution of supraventricular arrhythmia, and decrease in thyroid-stimulating hormone (TSH) and free-thyroxine (FT4) levels were achieved. In addition, attention-deficit hyperactivity disorder (ADHD) symptoms improved, with a concomitant decline in the ADHD Rating Scale score.
Summary: A TRIAC pharmacokinetic study, conducted using triiodothyronine level as a surrogate for TRIAC level, demonstrated that TRIAC disappears from the circulation rapidly and has a shorter duration of TSH secretion inhibitory effect in the RTH patient compared to that in the control subject. Studies of TSH and FT4 levels over a period of 3 years indicated that the TRIAC effect is dose dependent.
Conclusions: TRIAC was effective and safe in ameliorating the effects of hyperthyroidism and ADHD symptoms in a child with known genetic RTH. Further, it was demonstrated that TRIAC has a short half-life and functions dose dependently.

Introduction

THYROID HORMONE RESISTANCE (RTH) is a hereditary disorder presenting with variable target tissue hyposensitivity to the metabolic actions of thyroid hormones (THs) (1–3). In about 85% of RTH cases, heterozygous mutations of the TH receptor (TR)-β gene (*THRB*) are found. Non-suppressed thyroid-stimulating hormone (TSH) in the presence of elevated TH concentrations is a uniform characteristic finding in RTH. According to clinical manifestations, the condition may be categorized as either generalized RTH (GRTH) or pituitary RTH (PRTH) (4,5). While most RTH patients belong to the GRTH class and exhibit a euthyroid goiter, PRTH patients present with a hypermetabolic state. For this rare form of hyperthyroidism, treatment with several kinds of agents, including antithyroid drugs (6–8), β-blockers, bromocriptine (9,10), octreotide (11), dextrothyroxine (7,12), and the triiodothyronine (T3) analog 3,5,3′-triiodothyroacetic acid (TRIAC), has been attempted. Among these, TRIAC seems to be most promising (10,13–19), even though some investigators have undervalued its clinical effects (7,9,20,21). Here, we report the favorable effects of a 3-year course of TRIAC therapy in a Japanese boy with PRTH, and the study of TRIAC pharmacokinetics. We discuss our results in terms of optimization of the TRIAC therapy regimen.

Patient report

The patient is a Japanese boy who was born without any complications at 37 weeks of gestational age. He weighed 2884 g (−1.6 standard deviation [SD]) at birth. He had an elder brother with childhood-type hypophosphatasia. Through fetal ultrasonography (US), the patient was found to have shortening of the extremities and was suspected to have

Departments of [1]Endocrinology and Metabolism and [2]Child and Adolescent Psychiatry, Kanagawa Children's Medical Center, Yokohama, Japan.
[3]Department of Pediatrics, Shimane University School of Medicine, Yonago, Japan.

hypophosphatasia. This diagnosis was later supported by elevated urinary excretion of phosphoethanolamine and by the identification of a common heterozygous mutation (c.1559delT) in the liver/bone/kidney alkaline phosphatase gene (*ALPL*). His motor development was slightly delayed; he could keep his head steady at 5 months, and he walked independently at 24 months. At 4 years, he suffered from right-sided Perthes' disease, which necessitated operative intervention. At this time, he was referred to us for evaluation of his short stature. Through the endocrinological work-up, the thyroid function tests showed unexpected results. The serum TSH level was 3.48 μIU/mL (reference range [RR]: 0.43–4.0 μIU/mL), the serum free-T3 (FT3) was 9.62 pg/mL (RR: 2.32–4.60 pg/mL), and the serum free-thyroxine (FT4) was 4.15 ng/dL (RR: 1.01–1.97 ng/dL). Clinical re-evaluation following the thyroid function tests revealed the presence of goiter. At this point, hyperthyroidism was not evident, except for mild tachycardia (heart rate, up to 102/min). RTH was suspected and was confirmed by the *TR-β* gene analysis that revealed a heterozygous P453T mutation.

From 5 years of age, tachycardia (heart rate, up to 120/min) was repeatedly recorded at outpatient visits. In addition, diaphoresis and repetitive diarrheal episodes had occurred. A child psychiatrist noted that he was hyperactive and impulsive despite normal intellectual development. Treatment with a β-blocker (propranolol, 0.5 mg/kg/day) was started under the diagnosis of PRTH, but it did not decrease the heart rate.

At 8 years of age, his parents sought a second consultation with the child psychiatrist, because the patient had exhibited recent disruptive behaviors such as frequent quarreling with classmates and throwing tantrums. According to the psychiatrist, he was maladaptive, and he presented with distinctive symptoms compatible with attention-deficit hyperactivity disorder (ADHD), such as hyperactivity, inattention, and impulsiveness. The extent of his ADHD symptoms was considered to be inconsistent to his reported intelligence quotient (IQ) of 79–89 (the method used for measuring the IQ is unknown). He did not show any symptoms indicative of autism.

TRIAC therapy was planned, and favorable effects were expected for both hyperthyroidism and ADHD symptoms. The patient was admitted for a short period for pretreatment endocrinological, cardiac, and metabolic evaluations. At the time of admission, he was 9 years old, 112.8 cm (−3.3 SD) tall, and weighed 20.8 kg (body mass index, 50th percentile). His blood pressure (BP) was 105/76 mm Hg, and body temperature was 36.0°C. His pulse rate (PR) was regular (80/min at rest), but it tended to increase frequently (up to 150/min) with light physical activity such as walking. Holter electrocardiography showed frequent supraventricular premature contraction (SVPC) during sleep. He was so hyperactive that he was not able to sit still. Excessive sweating was observed. The thyroid gland was diffusely enlarged and elastically soft on palpation. He did not show exophthalmia or finger tremor. He showed no pubertal development (Tanner stage: genital development 1 and pubic hair development 1), and his testicular volume was 2 mL on each side. Laboratory data were unremarkable, except for high TH levels (FT3 = 15.8 pg/mL, RR: 2.50–4.77 pg/mL; FT4 = 5.60 ng/dL, RR: 1.02–1.99 ng/dL) with nonsuppressed TSH (2.68 μIU/mL, RR: 0.46–4.4 μIU/mL). His total cholesterol level was 149 mg/dL (RR: 117–223 mg/dL), and his creatine phosphokinase level was 55 IU/L (RR: 53–283 IU/L). TRIAC was started at a dose of 0.2 mg/day, administered in two equally divided doses (at breakfast and supper). Except for transient nausea in the earlier phase of treatment, no severe adverse events were observed for the next 3 years with an increasing TRIAC dose. His last IQ, measured at 13 years of age, was reported to be 83.

Methods

Evaluation of TRIAC effectiveness

The therapeutic effects of TRIAC were initially monitored monthly and later every 3 months, in an outpatient setting. The patient usually visited in the evening, about 8 hours after administration of the morning TRIAC dose. After blood sampling, his BP and PR were recorded in the sitting position. TSH, FT3, FT4, T3, and thyroxine (T4) levels were measured at an in-house laboratory by electrochemiluminescence immunoassay (ECLIA). Holter electrocardiography and thyroid volume estimation by US were carried out annually. Any effects of the TRIAC treatment on ADHD symptoms were assessed based on the parents' observations. The ADHD Rating Scale-IV (22), translated into Japanese, was also scored by the parents. As the TRIAC dose was gradually increased, TSH and FT4 values were evaluated during each of the three periods during which he was given increasing doses of TRIAC in a stepwise fashion. During the initial 4 months, he received TRIAC, 0.7–1.0 mg/day. During the next 4 months, he was given TRIAC, 1.5–2.5 mg/day, and during the last 18 months, he was given TRIAC, 3.0 mg/day.

Spiked recovery test to determine if serum T3 levels reflect serum TRIAC levels

During TRIAC therapy, the values for the patient's serum T3 level increased to above the range of the T3 assay. We hypothesized that this was due to crossreactivity of TRIAC with T3 in the T3 ECLIA. To determine the extent to which serum T3 reflects the serum TRIAC level, we tested the recovery of added TRIAC in T3 assay. Increasing doses of TRIAC (5, 10, 20, 40, and 80 ng) were added to 10 mL of pooled serum. In each sample, concentrations of T3 and T4 were measured by ECLIA (Elecsys® T3 and T4; Roche Diagnostics, Tokyo, Japan) and chemiluminescent immunoassay (CLIA) (Chemilumi E-T3® and Chemilumi ACS-T4®; Siemens Healthcare Diagnostics, Tokyo, Japan). Antibodies used in ECLIA and CLIA were ovine polyclonal and murine monoclonal antibodies, respectively. The same procedure was performed using hypothyroid serum (T3 0.39 ng/mL and T4 0.76 μg/dL) instead of pooled serum. All assays were conducted in duplicate. The recovery rate was expressed as the percentage of the observed increment in T3 concentrations to the expected values. Table 1 summarizes the assay kits used in this report.

Pharmacokinetic study of single TRIAC dose

As a control for these studies, 1.0, 2.0, and 4.0 mg of TRIAC were administered to a normal adult male volunteer on separate occasions. Serum samples were obtained before and 1, 2, 3, 6, and 24 hours after the administration of TRIAC, and samples were assayed in the T3 ECLIA. For the sera, which showed readings for T3 above the measurable range, T3 was measured after dilution with hypothyroid serum, and the measured value was then converted appropriately. The TSH level in each sample was also determined. For determination

TABLE 1. ASSAY KITS FOR THYROID HORMONE MEASUREMENTS USED IN THIS REPORT

Target hormone: Purpose	*Commercial kit used*	*Measurement technique*
Total T3:		
Clinical use; evaluation of TRIAC crossreactivity	Elecsys® T3	ECLIA
Evaluation of TRIAC crossreactivity only	Chemilumi E-T3®	CLIA
Total T4:		
Clinical use; evaluation of TRIAC crossreactivity	Elecsys® T4	ECLIA
Evaluation of TRIAC crossreactivity only	Chemilumi ACS-T4®	CLIA
Free T3: Clinical use only	Elecsys® FT3II	ECLIA
Free T4: Clinical use only	Elecsys® FT4	ECLIA

CLIA, chemiluminescent immunoassay; ECLIA, electrochemiluminescence immunoassay; T3, triiodothyronine; T4, thyroxine; TRIAC, 3,5,3′-triiodothyroacetic acid.

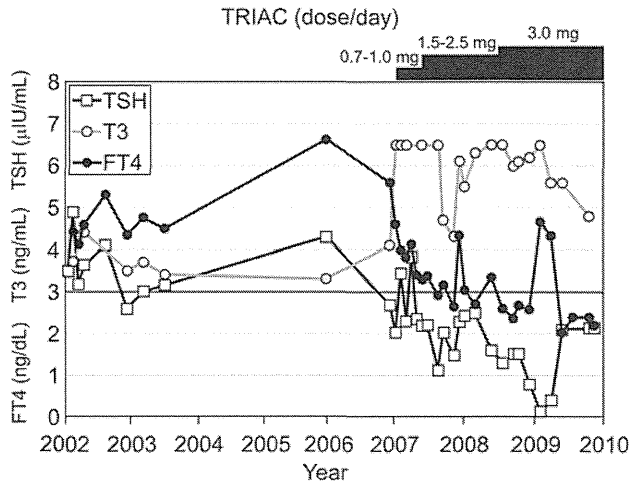

FIG. 1. Thyroid function tests conducted on the patient before and during 3 years of TRIAC therapy. TRIAC, 3,5,3′-triiodothyroacetic acid; TSH, thyroid-stimulating hormone; FT4, free thyroxine; T3, triiodothyronine.

of T3 and TSH levels, samples were assayed in duplicate. Our RTH patient also underwent this study for 3 years after the initiation of TRIAC, at which time he was 12 years old and weighed 29 kg. He received 1.5 mg of TRIAC in the morning, and serum samples were obtained 0, 1, 2, 3, 6, 12, and 24 hours later for T3 and TSH determination.

Statistical analysis

Statistical analysis was carried out using Microsoft Office Excel 2007® (Microsoft Corporation, Tokyo, Japan) and Statcel® (an add-in forms feature on Excel, 2nd edition; OMS Publishing, Tokyo, Japan). Values are expressed as mean ± SD. Mean values of FT4 and T4 levels at the different TRIAC doses were compared by the Kruskal-Wallis test, followed by Bonferroni and Tukey-Kramer corrections. Results of the spiked recovery test were evaluated by linear regression analysis. Mean TSH levels before and 24 hours after single TRIAC administration were compared by Mann–Whitney *U*-test. *p*-values of less than 0.05 were considered to be significant.

Approval

The Ethics Committee of the Kanagawa Children's Medical Center reviewed and approved the study protocol. Written informed consent was obtained from the parents of the patient as well as from the volunteer who participated in the pharmacokinetic study.

Results

Clinical effectiveness of TRIAC

We aimed to maintain TSH levels, measured on clinic visits, below 3.0 μIU/mL, which was an arbitrarily set value. To achieve this target, we needed to raise the TRIAC dose gradually up to 3.0 mg/day (Fig. 1). Despite the gradual increase in the TRIAC dose, an occasional decrease in FT3 levels was noted, which was interpreted as inadequate patient compliance. Nevertheless, after TRIAC therapy, some favorable effects were noted. At first, shrinkage of the goiter was noticed at 3 months after TRIAC introduction. This was confirmed by consecutive US studies (Table 2). Although BP and PR did not vary significantly (data not shown), Holter electrocardiography demonstrated a decrease in the mean heart rate as well as the dissolution of SVPC (Table 2). Diaphoresis and diarrhea subsided soon after TRIAC therapy was started. Improvements in hyperactivity and impulsiveness were noticed by the parents around 6 months after TRIAC treatment was started. Disruptive behaviors were not reported thereafter. ADHD Rating Scale-IV showed a marked decrease in the scores over a 3-year period (Table 2). More than 85% of TSH values were below 3.0 μIU/mL, as originally aimed (Table 3). FT4 and T4 levels during the last 18 months (with TRIAC 3.0 mg/day) were significantly lower than those during the initial 4 months (with TRIAC 0.7–1.0 mg/day; Table 3).

Spiked recovery test findings

Figure 2 shows the relationship between the added TRIAC dose and the recovered TRIAC dose inferred by the increment of T3 levels measured by both ECLIA (with ovine polyclonal

TABLE 2. EFFECT OF TRIAC THERAPY ON CARDIAC, VOLUMETRIC, AND PSYCHIATRIC PARAMETERS

	Before TRIAC therapy	*During TRIAC therapy*	
		12 months	*36 months*
SVPC	Frequent	Not observed	2/24 h
Heart rate, mean (range)	105 (64–192)	100 (58–153)	82 (50–144)
Thyroid volume	18.6 mL	16.5 mL	9.0 mL
ADHD Rating Scale-IV	21	not done	9

ADHD, attention-deficit hyperactivity disorder; SVPC, supraventricular premature contraction.

TABLE 3. EFFECT OF TRIAC THERAPY ON THYROID FUNCTION TESTS

TRIAC dose	*0.7–1.0 mg/day*	*1.5–2.5 mg/day*	*3.0 mg/day*
TSH (mean±SD) [μIU/mL]	2.78±0.80 (n=5)	2.02±0.48 (n=8)	1.85±1.45 (n=12)
Free T4 (mean±SD) [ng/dL]	3.98±0.44 (n=5)	3.18±0.54 (n=8)	2.86±0.87[a] (n=11)
T4 (mean±SD) [μg/dL]	19.9±1.17 (n=5)	16.7±2.28 (n=8)	14.9±3.02[b] (n=10)

[a] $p<0.05$, compared to TRIAC dose of 0.7–1.0 mg/day.
[b] $p<0.01$, compared to TRIAC dose of 0.7–1.0 mg/day.
TSH, thyroid-stimulating hormone.

anti-T3 antibody) and CLIA (murine monoclonal anti-T3 antibodies). The values determined by ECLIA were almost two times higher than those determined by CLIA at all points. However, a close linear relationship with TRIAC concentrations was observed irrespective of the measurement method (ECLIA or CLIA) and the medium (pooled serum or hypothyroid serum). TRIAC crossreactivity was calculated as 79.0% (ECLIA, hypothyroid sera), 61.6% (ECLIA, pooled sera), 37.9% (CLIA, hypothyroid sera), and 32.5% (CLIA, pooled sera). T4 levels, as measured by both ECLIA and CLIA, were not influenced by the TRIAC spike (data not shown).

Pharmacokinetic study of single TRIAC dose

Based on the results of the spiked recovery test, changes in the serum TRIAC level after single administration of TRIAC were evaluated in a healthy adult volunteer using ECLIA T3 as a TRIAC surrogate. As depicted in Figure 3, T3 levels after treatment with 1–4 mg TRIAC peaked within 1–2 hours, and then returned to initial levels within 6 hours. In our patient, T3 levels peaked 1 hour after TRIAC ingestion. Serum TSH levels showed a continuous downward trend that lasted for 24 hours after TRIAC treatment in the healthy adult volunteer. In the patient, the TSH level was lowest at 6 hours after TRIAC treatment.

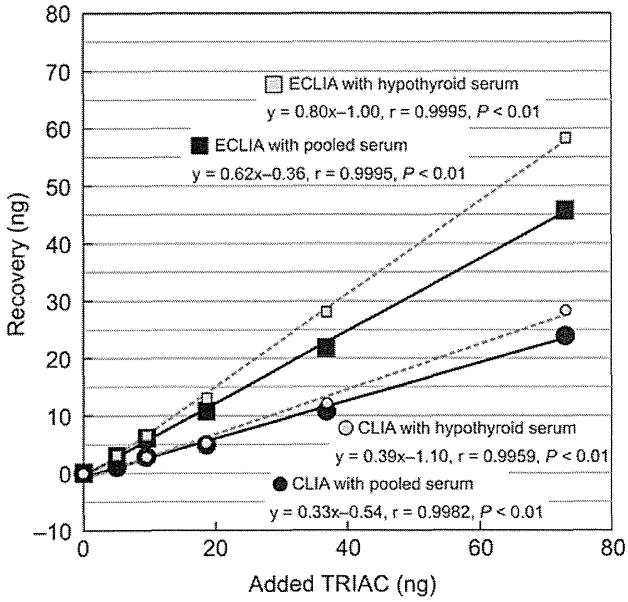

FIG. 2. Results of the spiked recovery test for TRIAC. Black symbols with solid lines indicate data obtained using pooled sera as medium. Gray symbols with dashed lines indicate data obtained using hypothyroid sera. CLIA, chemiluminescent immunoassay; ECLIA, electrochemiluminescence immunoassay.

Discussion

The heterozygous P453T mutation in the gene encoding TR-β has been identified in four GRTH kindred (23–26) and in one boy who was assumed to have hyperthyroidism (15). Our patient seemed to be in a hyperthyroid state based on his symptoms, which included diaphoresis, tachycardia, and repetitive diarrhea. Presentation of SVPC further supported this assumption, because atrial arrhythmia frequently occurs in hyperthyroid individuals (27). Although some RTH individuals have mixed symptoms of hyperthyroidism and hypothyroidism, our patient did not show any overt signs or biochemical indications of hypothyroidism. His short stature was considered to be due to hypophosphatasia. In addition, his cognitive ability did not seem to be severely impaired. Thus, our patient presented exclusively with the symptoms of hyperthyroidism, which was similar to the previously reported case of a boy with the same P453T mutation (15).

Effectiveness of TRIAC treatment in RTH patients has been investigated on a case-by-case basis with short treatment

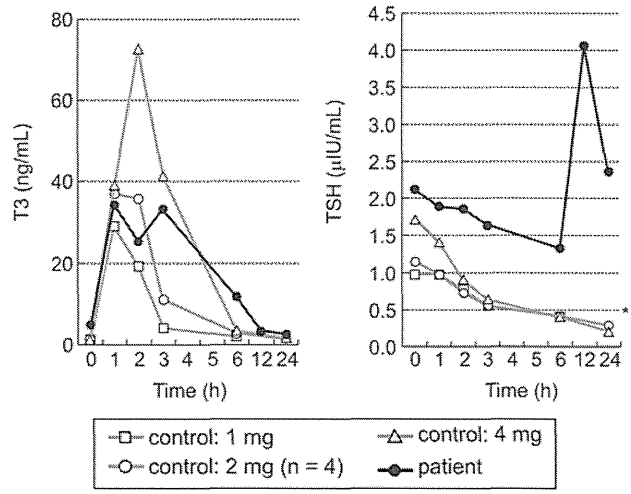

FIG. 3. T3 (left panel) and TSH (right panel) changes following a single TRIAC dose in a healthy control and the patient. A healthy adult volunteer ingested 1–4 mg of TRIAC on six separate occasions, whereas the patient ingested 1.5 mg of TRIAC. *TSH at 24 hours (n=5, 1.21±0.43) in the healthy volunteer showed a significant decrease compared to TSH at 0 hour (n=6, 0.27±0.08) ($p<0.01$).